Diffusing wave spectroscopy of dense colloids: Liquid, crystal and glassy states

SUBRATA SANYAL† and AJAY K SOOD*

Department of Physics, Indian Institute of Science, Bangalore 560 012, India
†Present address: Department of Chemical and Nuclear Engineering, University of California at Santa Barbara, Santa Barbara, CA 93106, USA
*Also at Jawaharlal Nehru Centre for Advanced Scientific Research, Jakkur Campus, P O Jakkur, Bangalore 560 064, India

Abstract. Using intensity autocorrelation of multiply scattered light, we show that the increase in interparticle interaction in dense, binary colloidal fluid mixtures of particle diameters $0.115\,\mu m$ and $0.089\,\mu m$ results in freezing into a crystalline phase at volume fraction ϕ of 0.1 and into a glassy state at $\phi = 0.2$. The functional form of the field autocorrelation function $g^{(1)}(t)$ for the binary fluid phase is fitted to $\exp[-\gamma(6k_0^2 D_{eff} t)^{1/2}]$ where k_0 is the magnitude of the incident light wavevector and γ is a parameter inversely proportional to the photon transport mean free path l^*. The D_{eff} is the l^* weighted average of the individual diffusion coefficients of the pure species. The l^* used in calculating D_{eff} was computed using the Mie theory. In the solid (crystal or glass) phase, the $g^{(1)}(t)$ is fitted (only with a moderate success) to $\exp[-\gamma(6k_0^2 W(t))^{1/2}]$ where the mean-squared displacement $W(t)$ is evaluated for a harmonically bound overdamped Brownian oscillator. It is found that the fitted parameter γ for both the binary and monodisperse suspensions decreases significantly with the increase of interparticle interactions. This has been justified by showing that the calculated values of l^* in a monodisperse suspension using Mie theory increase very significantly with the interactions incorporated in l^* via the static structure factor.

1. Introduction

Charged stabilized aqueous colloidal suspensions of polystyrene particles (polyballs) and sterically stabilized nearly hard sphere colloids of polymethyl methacrylate particles have proved to be model condensed matter systems to study a rich variety of cooperative behaviour in equilibrium and non-equilibrium conditions [1]. These systems show liquid, crystal and even glassy states under suitable experimental conditions. Monodisperse polyball suspensions show either a body-centered cubic (BCC) phase at low volume fraction ϕ or a face-centered cubic (FCC) phase at high ϕ. Small-angle neutron scattering measurements [2] of the structure factors reveal a glassy phase in these systems for $\phi > 0.2$. Monodisperse suspensions of polymethyl methacrylate particles have been studied extensively from the point of view of freezing of a liquid to an equilibrium crystalline phase or a metastable glassy state as a function of volume fraction ϕ [3–5].

In comparison with monodisperse suspensions, much less attention has been paid to the case of freezing of binary mixtures. The phase diagram becomes much richer

1

and complex with the introduction of two more parameters, namely, the diameter ratio $\sigma[=\sigma_A/\sigma_B, \sigma < 1]$ and the relative number density of the small particles $x[=n_A/(n_A + n_B)]$, to characterize binary mixtures. Several compound crystalline structures have been identified [6, 7] in the optical microscopy of concentrated ($\phi \sim 0.3$) aqueous suspensions of binary charged polystyrene spheres with diameters between 0.2 and 0.8 μm. The observed structures were similar to those found in the intermetallic compounds $MgCu_2$, AlB_2, $CaCu_5$, $NaZn_{13}$ and also of the type AB_4 with $P6_3/mmc$ symmetry, which has no counterpart in the conventional atomic systems. Bartlett *et al* [8] have studied the phase diagram of binary mixtures of nearly hard-sphere polyballs for some values of σ. These studies confirm the existence of AB_2 and AB_{13} superlattices in the (ϕ_A, ϕ_B) phase-diagram. In addition to the crystalline phase, glassy state has also been observed in polyball binary mixtures in measurements of shear modulus [9], static structure factor [10], diffusing wave spectroscopy [11] and Brownian dynamics simulations [12, 13]. The ease in the formation of glassy state in binary colloidal mixtures or charge-polydisperse colloids [12, 14] is similar to the fact that multicomponent solid solutions in conventional atomic systems are good glass formers [15].

Dynamics of the colloidal systems have been extensively studied by dynamic light scattering (DLS) experiments where the temporal fluctuations of the scattered light are analyzed in real time in terms of the intensity autocorrelation functions [16, 17]. In using the DLS technique, a stringent requirement is that the incident radiation should by scattered only once in the medium. Multiple scattering is avoided either by matching the refractive indices of the particles and the solvent [5] or by taking a low concentration of particles or thin sample cells. DLS measurements of the intermediate scattering functions have yielded valuable information on the non-ergodicity parameters across the kinetic glass transitions [4] allowing a direct comparison with the mode-coupling theory predictions [18].

The recently developed technique of the diffusing-wave spectroscopy (DWS) [19–22] has made it possible to study the particle dynamics from the intensity correlation functions in concentrated interacting suspensions. Subsequently, useful information about the polarization dependence in the freezing of monodisperse polyball suspensions [23] and also about the particle diffusion in the binary polyball mixtures are obtained by using DWS [24]. During the course of our studies, using DWS experiments on binary mixtures of strongly interacting polyballs, Meller and Stavans [11] have reported comprehensive phase diagrams (ϕ versus x) consisting of liquid, crystalline and glassy states for three values of σ, namely, 0.54 ± 0.02, 0.78 ± 0.04 and 0.87 ± 0.03. The different states of the system were confirmed from the presence or absence of Bragg-iridescence from the samples and the long-time temporal decay or saturation of the intensity autocorrelation functions. Our Brownian dynamics (BD) simulations [13] on binary mixtures, with $\sigma = 0.495$ and $x = 0.5$, reveal a liquid to crystal transition at $\phi \sim 0.2$ and a liquid to glass transition at $\phi \sim 0.3$. This is quite different from the results read from Meller and Stavans's [11] phase diagram with the parameters closest to our simulation, namely, $\sigma = 0.54 \pm 0.02$ and $x = 0.5$. In their experiments [11], the mother samples of 10% volume fraction were treated with ion-exchange resins to reduce the impurity ion concentration n_i till these showed strong crystalline iridescence. The samples with different ϕ and x, on which the measurements were performed, were then made out of these mother samples. In the simulations, on the

contrary, the n_i of the binary liquid phase at each ϕ is successively reduced to increase the interparticle interaction in the system. To confirm that the difference between the DWS and the BD simulation results are indeed due to the difference in the sample preparations in the two cases, one must carry out DWS experiments and look for the liquid to crystal and the liquid to glass transitions on concentrated binary polyball mixtures, prepared similarly as in the simulation. This is the motivation of the present work. We indeed find, in accordance with our simulation [13], that a binary liquid mixture freezes into a crystalline phase at a lower volume fraction ($\phi = 0.1$), while it forms a glassy state at $\phi = 0.2$. Along the way, the DWS intensity autocorrelation functions of the binary liquid phase were analyzed in terms of effective diffusion constants [22], wherein the transport means free path, l^* [25], has been incorporated using the Mie scattering theory [26]. The slope parameter γ, to be explained in the following subsection [eq. (9)], shows a systematic dependence on the interaction between the particle. This has been understood by realizing that γ is inversely proportional to l^*, which increases with the interaction strength.

2. Theoretical background

DWS extends DLS to the optically turbid media and relates the temporal fluctuations of the multiply scattered light to the motion of the scatterers. The transport of photon is assumed to be diffusive with a diffusion constant $D_l = cl^*/3$, where c is the velocity of light in the medium. The transport mean free path l^* is related to the scattering mean free path l (the mean distance between successive scattering events) by $l^*/l = 2k_0^2/\langle q^2 \rangle$, where k_0 is the photon wave vector in the medium and $\langle q^2 \rangle$ is the mean squared scattering wave vector. The normalized temporal field autocorrelation function is defined by

$$g^{(1)}(q,t) = \frac{G^{(1)}(q,t)}{G^{(1)}(q,0)} \equiv \frac{\langle E_s(q,0)E_s^*(q,t) \rangle}{\langle |E_s|^2 \rangle}. \tag{1}$$

Within DWS, for the noninteracting monodisperse Brownian particles, it is given by [22]

$$g^{(1)}(q,t) = \int_0^{\infty} P(s)e^{(-2t/\tau_0)s/l^*} ds, \tag{2}$$

where $P(s)$ is the distribution of path-lengths s for the random walk of photons and

$$\tau_0 = \frac{1}{Dk_0^2}. \tag{3}$$

Here D is the free particle diffusion coefficient.

For the "backscattering" geometry and the source at a fixed distance, $z_0 \sim l^*$, inside from the illuminated face at $z = 0$ of a slab of thickness L, one obtains [22]

$$G^{(1)}(t) = \frac{\sinh\left[\sqrt{\frac{6t}{\tau_0}}\left(\frac{L}{l^*} - \frac{z_0}{l^*}\right)\right] + \frac{2}{3}\sqrt{\frac{6t}{\tau_0}}\cosh\left\{\sqrt{\frac{6t}{\tau_0}}\left(\frac{L}{l^*} - \frac{z_0}{l^*}\right)\right\}}{\left(1 + \frac{8t}{3\tau_0}\right)\sinh\left[\frac{L}{l^*}\sqrt{\frac{6t}{\tau_0}}\right] + \frac{4}{3}\sqrt{\frac{6t}{\tau_0}}\cosh\left[\frac{L}{l^*}\sqrt{\frac{6t}{\tau_0}}\right]}. \tag{4}$$

For a sample of infinite thickness ($L \to \infty$), (4) simplifies to

$$G^{(1)}(t) = \frac{e^{-(z_0/l^*)(6t/\tau_0)^{1/2}}}{1 + \frac{2}{3}\sqrt{\frac{6t}{\tau_0}}}. \tag{5}$$

A distribution in the position z_0 of the source results in the replacement of z_0/l^* by $\langle z_0 \rangle/l^*$. It has been found experimentally that the $g^{(1)}(t)$ can be simply described using [19, 20]

$$g^{(1)}(t) = \exp[-\gamma(6t/\tau_0)^{1/2}], \tag{6}$$

where $\gamma = \langle z_0 \rangle/l^* + 2/3$, i.e., $\gamma \propto 1/l^*$ [22]. When $l^*/l = 10$, then $\gamma \simeq 2$ for both polarized and depolarized scattering [27].

For the case of interacting particles, Mackintosh and John [27] have shown that $g^{(1)}(t)$ is related to the dynamic structure factor $S(q, t)$ such that $2t/\tau_0$ in (2) is replaced by $(l^*/l)[1 - S(q, t)/S(q, 0)]$ where $S(q, t)$ is defined by

$$S(q, t) = \left\langle \frac{1}{N} \sum_{\alpha\beta} \exp[i\mathbf{q}\cdot(\mathbf{r}_\alpha(t) - \mathbf{r}_\beta(0))] \right\rangle \tag{7}$$

For short times, $S(q, t)$ can be expanded to linear power in t and hence it amounts to replacing t/τ_0 by t/τ'_0 where $\tau'_0/\tau_0 = \langle q^2 S(q) \rangle/\langle q^2 \rangle$ [22]. Thus the time scale of the decay of $g^{(1)}(t)$ is modified and its functional form (i.e. square root singularity) for short times is not affected by interactions.

The form of $g^{(1)}(t)$ for all times has been obtained [27] only under the simplifying assumption that the interparticle spacing is larger than the wavelength and the particle size, so that the particle vibrations in a colloidal crystal or a glass, around their mean positions may be considered independent of each other. In addition, due to the viscosity of the fluid, phonon-like motions are strongly overdamped. They have also assumed large wavevector transfers q which correspond to distances smaller than the mean interparticle spacing. With these simplifying assumptions, for the long paths, for which the scattered light is still diffusive, the dynamic structure factor is replaced by its self-part $S_s(q, t)$ given by

$$S_s(q, t) = \left\langle \frac{1}{N} \sum_{\alpha} \exp[i\mathbf{q}\cdot(\mathbf{r}_\alpha(t) - \mathbf{r}_\alpha(0))] \right\rangle \tag{8}$$

$$\simeq \exp(-W(t)q^2)$$

where $W(t)$ is the mean square displacement (MSD) of a particle in time t. Then

$$g^{(1)}(t) = \exp[-\gamma(6k_0^2 W(t))^{1/2}], \tag{9}$$

Since $W(t)$ shows a non-decaying part at long-times in a solid, eq. (9) will predict a non-zero $g^{(1)}(t)$ at large times for both polarized and depolarized scattered light.

The MSD can be evaluated by considering a model for the interacting Brownian particles. For a one-dimensional harmonically bound Brownian particle of mass M and diameter $\sigma_p = 2a_p$, suspended in a solvent of viscosity η, the velocity auto-correlation

function in the strongly overdamped case $(\beta/\omega \gg 1)$ is given by [16]

$$\Phi(t) \equiv \langle V(0) \, V(t) \rangle = \frac{k_B T}{M} \left[\exp(-\beta t) - \left(\frac{\omega^2}{\beta^2}\right) \exp\left(\frac{-\omega^2 t}{\beta}\right) \right], \tag{10}$$

where ω is the angular velocity associated with the harmonic potential, $\beta = \tau_v^{-1}$ with $\tau_v = M/6\pi\eta a_p$ as the Brownian velocity fluctuation time. This model applies strictly to the motion of a single particle in a colloidal crystal if the combined interparticle forces are treated in a harmonic approximation. It has been suggested [16] that the model can also be applied to the liquid-like ordering, if the similar form for the velocity autocorrelation function is retained, i.e.,

$$\Phi(t) = \frac{k_B T}{M} \exp\left(-\frac{t}{\tau_v}\right) - A \exp\left(-\frac{t}{\tau_I}\right), \tag{11}$$

where one expects that $A \ll k_B T/M$ and the fluctuation time associated with the interaction forces $\tau_I \gg \tau_v$. Within this model for times $t \gg \tau_v$, the MSD is given by

$$W(t) = Dt - A\tau_I(t + \tau_I \exp\{-t/\tau_I\} - \tau_I), \tag{12}$$

where the parameter A satisfies $A\tau_I < D$.

Let us now discuss DWS from a binary colloidal systems with species of different sizes. It has been shown that for noninteracting particles, the $g^{(1)}(t)$ is given by (2), where τ_0 [eq. (3)] is replaced by τ_{eff} [22],

$$g^{(1)}(t) = \exp(-\gamma(6t/\tau_{\text{eff}})^{1/2}), \tag{13}$$

where

$$1/\tau_{\text{eff}} = D_{\text{eff}} k_0^2,$$

$$D_{\text{eff}} = \left(\sum_i D_i/l_i^*\right) \Big/ \left(\sum_i 1/l_i^*\right). \tag{14}$$

The effective diffusion constant D_{eff} is the weighted average of the individual diffusion coefficients of the pure species, the values of which are calculated via Stokes' law [28], i.e., $D_i = k_B T/(6\pi\eta a_i)$ where η is the viscosity of water ($= 0.01089$ P) and a_i are the radii of the particles. The weighting factors in (14), i.e., the inverse transport mean free paths $1/l_i^*$ for the individual pure species are summed to yield the optical analogue of the resistivity of the binary liquid alloy [29]

$$1/l_{\text{eff}}^* = \sum_i 1/l_i^*. \tag{15}$$

As stated above, the key quantity within the diffusion approximation of the photon transport is the photon random-walk step length l^*, which depends on the number of scattering events needed to randomize the direction of photon. The number of scattering events, in turn, depends on the scattering properties of the individual particles as well as the interparticle spatial correlations [21, 22]. A general expression for l^* for the monosized particles calculated [21, 30, 31] within the Mie theory [26] is summarized in the Appendix.

In the laboratory, one measures the normalized temporal intensity autocorrelation function $g_2(t)$ which is related to $g^{(1)}(t)$ by the Siegert's relation, i.e.,

$$g_2(t) \equiv g^{(2)}(t) - 1 = f|g^{(1)}(t)|^2] \tag{16}$$

The parameter f is fixed by the system optics and can be taken as a free parameter in fitting (6) and (16) to the relevant data.

3. Experiments

We use aqueous suspensions of charged polystyrene spheres (M/s Seradyn Inc., USA) of diameters $\sigma_B = 0\cdot115\,\mu m$ and $\sigma_A = 0\cdot089\,\mu m$. The quoted standard deviation of the diameters is less than 1%. Two sets of samples are prepared from these mother solutions. In one set, the samples of the small and the large spheres are obtained independently from their respective mother solutions by adding required amounts of triple-distilled, deionized water, so that the final volume-fraction of each of them becomes $\phi_A = \phi_B = 0\cdot05$. Equal volumes of these samples are then mixed to get total $\phi = 0\cdot1$ in a cylinderical quartz scattering cell of 8 mm inner-diameter containing a mixed-bed of ion-exchange resins [AG501–X8(D), M/s Bio-Rad Inc., USA] at the bottom of the cell to reduce the coion concentration n_i. The cell is then closed air-tight with properly cleaned teflon cap and parafilm. In the other set, the mother samples of the small and the large spheres with $\phi_A = \phi_B = 0\cdot1$ are mixed in 1:1 volume-ratio (total $\phi = 0\cdot2$) in a similar quartz sample cell with ion-exchange resins. The volume-fractions of the constituent solutions were confirmed to be within an experimental accuracy of 5% by drying a known volume of the suspension and weighing the solids. After an initial vigorous mixing of the samples with the resins, the cells are transferred into their respective quartz glycerin baths and left undisturbed for about an hour before the data accumulation begin. This is necessary to assure a proper gravitational settling down of the resins in the cell as well as uniformity of the glycerin without any air-bubbles surrounding the cell. A linearly polarized beam from Kr^+ laser ($\lambda = 647\cdot1$ nm) falls on one side of the sample and the scattered light of desired polarization is collected from the same side (scattering angle $\theta = 165°$). The normalized intensity autocorrelation $g_2(t)$ [eq. (16)] is measured using the Malvern correlator (model 7032CE). The laser light is vertically (V) polarized. The emergent multiply scattered light has, in general, a polarized (vertical) component with intensity $I_V(t)$ and a depolarized (horizontal) component with intensity $I_H(t)$. By setting the orientation of the analyzer, $g_2(t)$ was measured in either polarized, i.e., $C_{VV}(t) \equiv \langle I_V(t)I_V(0)\rangle/\langle I_V\rangle^2 - 1$ or depolarized, i.e., $C_{VH}(t) \equiv \langle I_H(t)I_H(0)\rangle/\langle I_H\rangle^2 - 1$ component. We note that although in normal isotropic systems the measured correlation functions $C_{VV}(t)$ and $C_{VH}(t)$ behave in qualitatively the same way, they give us access to different physical properties. While both respond to translational motion [23, 27, 32], only C_{VH} is sensitive to changes in the local dielectric anisotropy and hence contains information about the correlations of orientational fluctuations as well. The field autocorrelation $g^{(1)}(t)$ in the backscattering geometry is extracted using Siegart's relation eq. (16).

We note that since the system is in a frozen but disordered (i.e. non-ergodic) state, we are obliged to average over space as well as time to sample a representative fraction of all the configurations. To this end, we have averaged the correlation functions obtained

from ten spatially separated regions in the suspension. Each of these regions is achieved simply by rotating the sample cell in its position. The curves so obtained are labelled ensemble-averaged, while those from a single region are called time-averaged.

4. Results and discussions

Our fluid-phase data for the total $\phi = 0 \cdot 1$ mixtures of the small and the large polyballs, before putting in the ion-exchange resins, are shown by open symbols in figure 1. The measured $g_2(t)$ were non-linear least-square fitted by a simulated annealing Monte Carlo fitting method [33] using (16) and (13) with f and γ as fitting parameters. The values of D_i, l_i^* (as calculated [34] from the Mie theory) for the two constituent particle suspensions and also the values of D_{eff}, are presented in table 1. The τ_{eff} was calculated using (14). The values of the fitting parameters are given in the table 2. Given the fitted value of f, the data have been presented in the form of normalized $g^{(1)}(t)$ (experimental $g^{(1)}(t)/f$) in figure 1. The values of the parameter γ for the polarized and depolarized scattering are comparable with those in the monodisperse colloids [22,23,32]. The polarization dependence of γ can be simply understood as follows [22]. The autocorrelation
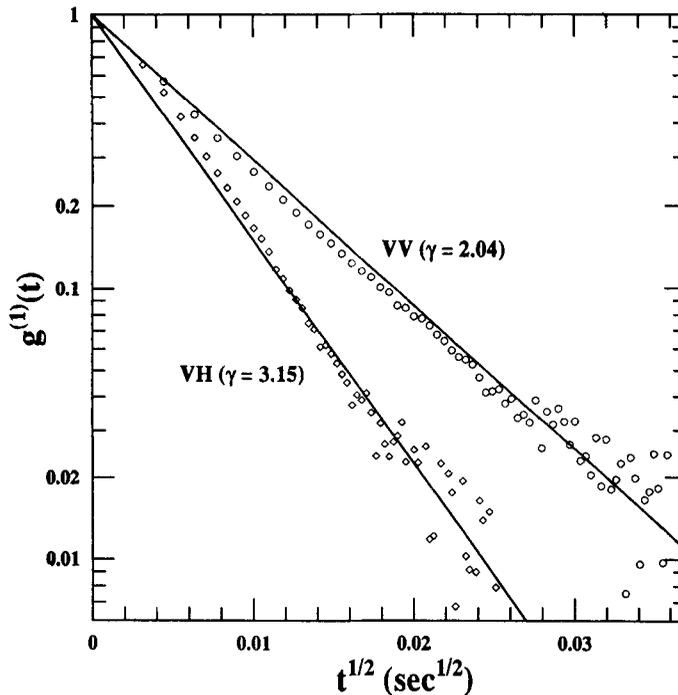

Figure 1. The fluid-phase time-averaged data for the polarized (VV) and the depolarized (VH) field autocorrelation functions $g^{(1)}(t)$ versus $t^{1/2}$ in the backscattering geometry from a binary mixture with $\sigma_A = 0 \cdot 089$ μm and $\sigma_B = 0 \cdot 115$ μ diameter polyballs at total $\phi = 0 \cdot 1$. The solid line through the data is the fit with eqs (11)–(13). The fitting parameters as given in tables 1 and 2.

Table 1. The parameters relevant to the Mie theory fits in figure 1 and the inset of figure 3, with $k_0 = 1297724 \, cm^{-1}$. The parameters σ_i and l_i^* are in μm, while the D_i or D_{eff} are in $10^{-8} cm^2/s$.

σ_i	D_i	l_i^*	D_{eff}
0·089	3·17	232·77	
			3·58
0·115	4·10	295·82	

Table 2. The fitting parameters corresponding to figures 1 to 5, with $k_0 = 1·29 \times 10^5 \, cm^{-1}$. Samples I and II are 1:1 binary mixtures of $0·115 \, \mu m$ and $0·089 \, \mu m$ diameter particles with total $\phi = 0·1$ and $0·2$, respectively. The monodisperse sample III has $\phi = 0·03$ and diameter $0·115 \, \mu m$. The D_{eff} is in units of $10^{-8} cm^2/s$, A in units of 10^{-5}, τ_1 in units of $10^{-3} s$. Liquid: L, Crystal: C, Freezing: F and Glass: G, Pol: polarization.

Sample	State	Pol	D_{eff}	A	τ_1	f	γ
I	L	VV	3·578	—	—	0·9	2·0367
I	L	VH	3·578	—	—	0·9	3·1537
I	F	VV	3·578	1·116	3·204	0·118	0·0932
I	F	VH	3·578	0·4456	8·029	0·317	0·1072
I	C	VV	3·578	0·6348	5·526	0·145	0·0203
I	C	VV	3·578	5·217	6·822	0·196	0·0762
II	L	VV	3·217	—	—	0·8	2·332
II	L	VH	3·217	—	—	0·8	3·763
II	G	VV	3·217	0·1046	30·723	0·226	0·0018
II	G	VH	3·217	1·2492	2·349	0·237	0·0049
III	L	VV	3·473	—	—	0·99	1·89
III	L	VH	3·473	—	—	1·06	2·87
III	F	VV	3·473	1·816	1·912	0·7	0·988
III	C	VV	3·473	1·732	1·990	0·6	0·723
III	C	VH	3·473	5·926	0·5817	0·6	0·463

function for the perpendicular polarization (VH) decays more rapidly because the analyzer discriminates against the short photon paths which retain a high degree of their incident polarization. On the other hand, the autocorrelation function for the parallel polarization decays more slowly, due to the additional contributions of the low order scattering paths which have a longer decay time. In other words, for very short-times (shorter than that shown in figure), $g^{(1)}(t)$ is dominated by long paths for which the observed photons have lost their memory of their incident polarization and hence C_{VV} and C_{VH} will initially decay at the same absolute rate. This means $(C_{VV} - C_{VH})$ will be independent of time to first order in $\sqrt{t}$. Since the short paths tend not to alter the polarization of the incident light, I_{VV} is in general higher than I_{VH} [in our experiments $I_{VV}/I_{VH} \sim 3$].

After these initial measurements, the samples cells are left undisturbed. Typically about 2 days later, the $\phi = 0{\cdot}1$ mixture started showing Bragg-iridescence in the immediate vicinity of the ion-exchange resins-bed. The crystalline region started growing slowly till the whole of the sample in the cell showed the iridescence. Under this condition, the correlation functions measured for different polarization channels are presented in figure 2, for two cases namely, (a) in the region of $1{\cdot}5$ mm above the top of the resins-bed at around 174 h after the addition of resins (sample I, state C in table 2) and (b) at the height of 4 mm from the top of the resins-bed and time 194 h (sample I, state F in table 2). The temporal correlation functions for different polarization channels follow the similar trends in the crystallizing samples. The form of the correlation function $g^{(1)}(t)$ is same as predicted by (9). We note that the mean interparticle spacing is almost one third of wavelength of light and hence the assumption of retaining only the self part of the structure factor in deriving (9) is not fully satisfied. However, since (9) is the only closed form expression available for the $g^{(1)}(t)$ for the interacting colloids, we have chosen to use it to fit our experimental data to get some estimates of the parameters γ, f, A and τ_1. The solid lines show the fit to (9) and (12) by varying f, τ_1, γ and A. The values of the fitting parameters are provided in the respective figures as well as in table 2. Given the value of f, here too the data are presented in the normalized form $g^{(1)}(t)$. We note that the fits, though excellent at long times, are not
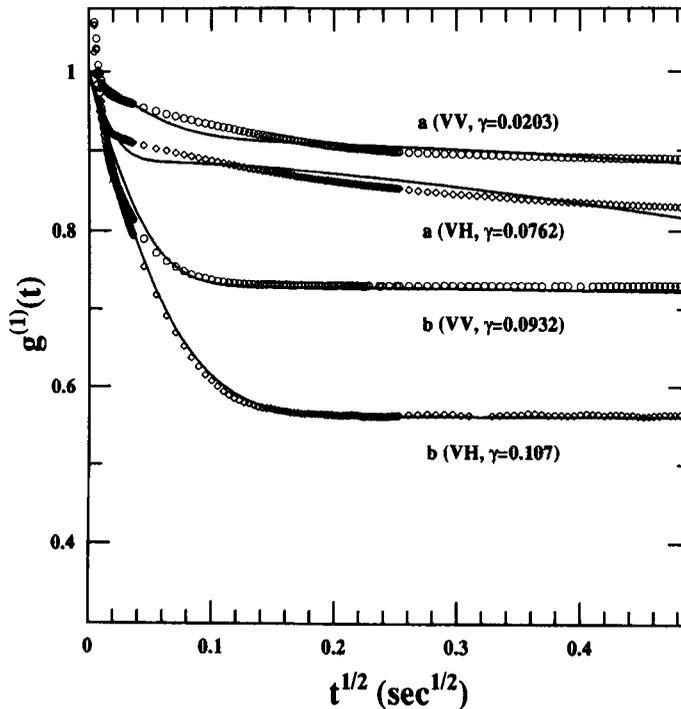

Figure 2. The normalized $g^{(1)}(t)$ versus $t^{1/2}$ for the different stages of crystallization in sample I ($\phi = 0{\cdot}1$) table 2. The data are shown in (a) the frozen state (state C, table 2) and (b) while freezing (state F, table 2). The solid lines are the fits to eqs (7) and (10). The fitted parameters are given in table 2.

so good at short times and hence the normalized data for $g^{(1)}(t)$ are slightly higher than 1 at short times.

The situation is quite different with the total $\phi = 0.2$ mixture. The sample does not show Bragg-iridescence even a few weeks after the addition of resins. The autocorrelation functions measured after a week from the addition of resins (figure 3) show significant non-zero values at long time, similar to that shown in figure 2. The absence of Bragg-iridescence and non-decaying intensity autocorrelation functions show that the particles are trapped in a disordered state, as in a conventional glass. For comparison, the inset shows the liquid state data for the sample (total $\phi = 0.2$) but at a high impurity concentration. Here again, the solid lines are the best fits to the data using (13) with f and γ as fitting parameters for the liquid state data in the inset and using (9) and (12) (by varying f, τ_1, γ and A) for the glass data. The relevant fitting parameters are listed in table 2. The quality of fit is poor at short time and hence the extracted normalized $g^{(1)}(t)$ is again slightly higher than unity for the glass data. Hence our experiments clearly show that the binary mixture with a total $\phi = 0.1$ freezes into a crystalline state whereas for $\phi = 0.2$, the interacting state of the mixture does not show a crystalline phase even after a few months and is best described as a glass. This observation is similar to the predictions of our simulation work [13]. As mentioned earlier, the difference between our results and those of Meller and Stavans [11] lies in the way the interaction is allowed to build up in the samples.
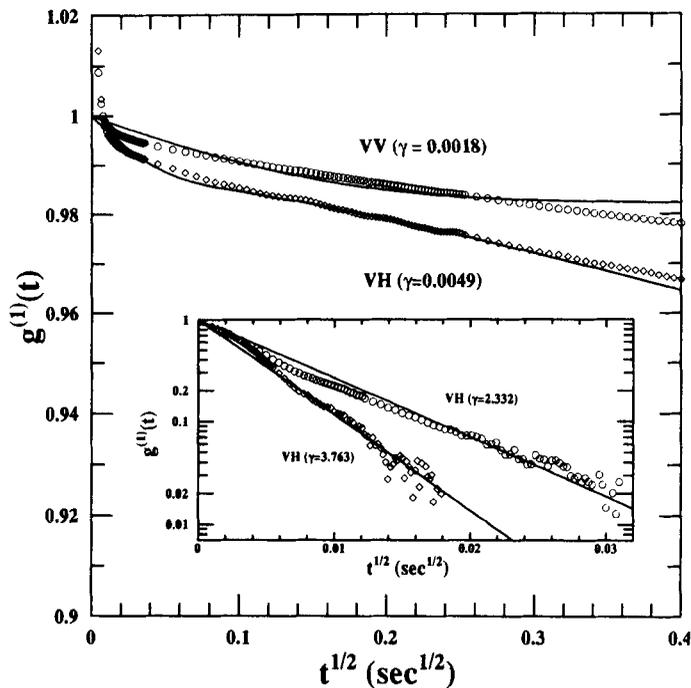

Figure 3. Same as in figure 2, but for the glass state with total $\phi = 0.2$ at the height of 4 mm from the top of the resins-bed and 171 h after the addition of resins. The inset shows the data and the fits for the corresponding noninteracting limit.

It is interesting to compare the values of the parameter γ in table 2 obtained in the interacting colloids with the corresponding values in the noninteracting limit (figure 1 and the inset of figure 3). We note that γ (for a given scattering geometry) decreases as the interaction between the particles increases towards forming a crystal or a glass. To ascertain that this is a property of the freezing suspensions, we show the ensemble-averaged $g^{(1)}(t)$ for a monodisperse suspension (diameter $\sigma_p = 0.115\,\mu m$ and volume fraction $\phi = 0.03$) in figure 4. The panel (a) shows the data for the parallel polarization channel (i.e. VV) of the system while freezing and the panel (b) shows both the parallel (VV) and the perpendicular (VH) channels in the state when the suspension has completely frozen into a crystalline order. In the state of freezing, as shown in figure 4(a), the sample shows the polarization dependence [23] of the correlation functions i.e., C_{VH} shows a liquid-like curve and hence the corresponding $g^{(1)}(t)$ is not plotted. The value of the parameter γ indeed decreases with the interaction as can be seen clearly by comparing figure 4 with the fluid-phase data shown by open circles and diamonds in figure 5 (see also table 2). In figure 5, we have also compared these with the initial part of the VV data in the crystallizing state (shown by $+$). We see clearly that as the interparticle interaction becomes important, the decay of $g^{(1)}(t)$ is different from
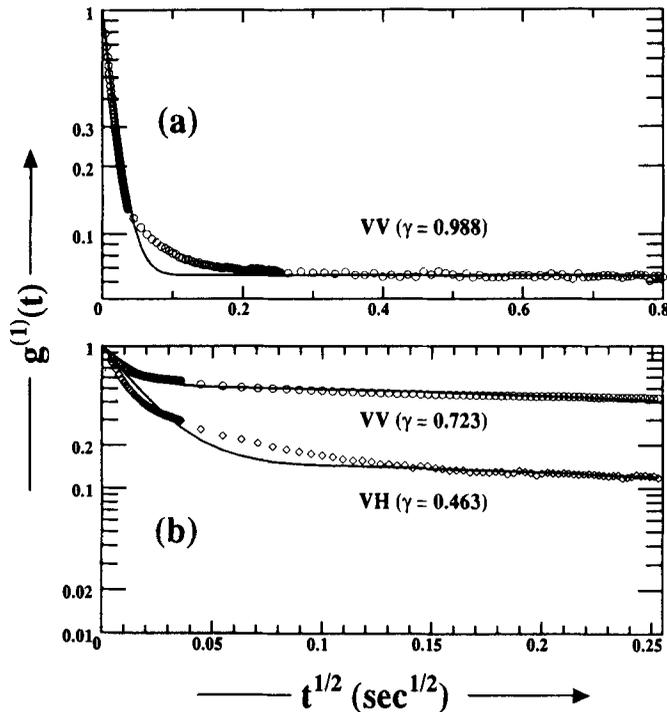

Figure 4. The semilog plots of the ensemble-averaged $g^{(1)}(t)$ versus $t^{1/2}$ (in $sec^{1/2}$) of $0.115\,\mu m$ polyball suspension with $\phi = 0.03$ (a) while freezing and (b) in the crystalline state alongwith the fits (solid lines) to a harmonic model as explained in the text, with parameters in table 2.
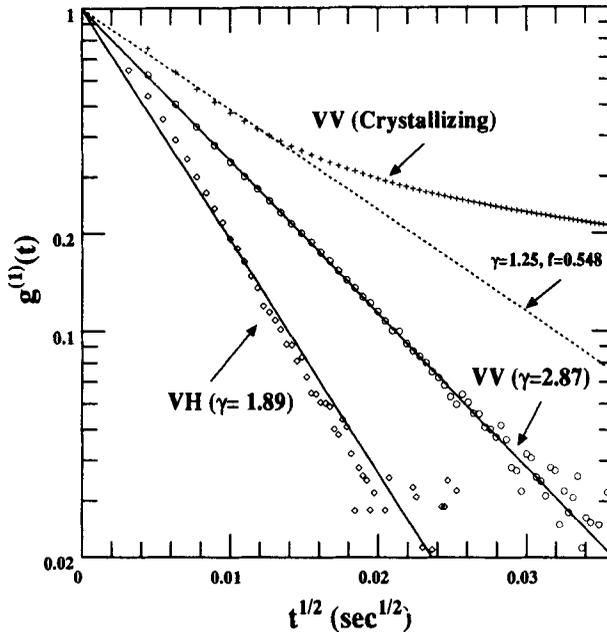
Figure 5. The fluid phase VV and VH time-averaged $g^{(1)}(t)$ versus $t^{1/2}$ (in $sec^{1/2}$) for $\phi = 0.03$ is compared with the initial times data in the crystallizing state.

that without interaction, even at very early times. This is demonstrated by fitting (6) to the first 10 data points of the crystallizing suspension, shown by the dashed line and the corresponding parameters are given in table 2.

As we have mentioned before, the parameter γ is inversely proportional to the transport mean free path l^*, i.e., $\gamma \propto 1/l^*$ [22]. Therefore, the result that the magnitude of γ reduces with the growth of interaction in the system can be justified if we can show that l^* increases with the interaction. We do this only for the *monodisperse suspensions* (see Appendix for details). We calculate the l^* [eq. (17) of Appendix] by using the form factor $F(q)$ from the Mie scattering theory [eq. (18)] and incorporate the interparticle interaction through the structure factor $S(q)$ which can be calculated using either rescaled mean spherical approximation or Percus–Yevick approximation. For the present purpose, it suffices to note that the interacting charged colloids can be approximated to effective hard spheres by rescaling the volume fraction and therefore the Percus–Yevick approximation for the hard sphere system for which analytical results are known has been used as an input $S(q)$ in (17). The PY approximation, though not as good as mean spherical approximation for the $S(Q)$ of colloids, has been used because of the simple closed form expression [see (21) of the Appendix]. Our purpose is only to show qualitatively that l^* increases with the strength of interactions. In figure 6 we have shown the Percus–Yevick $S(q)$ for nine such different rescaled volume fractions ϕ^*. The height of the first peak of the structure factor, S_{max}, can be taken as a scale to measure the interparticle interaction. Figure 7 represents the calculated values of l^* for these $S(q)$ as a function of the interparticle interaction measured by S_{max}. We clearly see
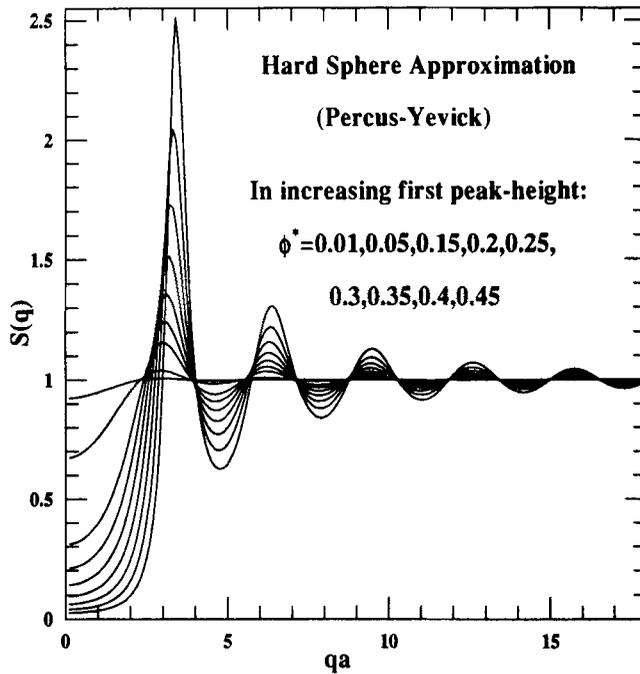
Figure 6. The static structure factor $S(q)$ in the Percus–Yevick approximation as a function for ten different values of the effective hard sphere volume-fraction ϕ^*.
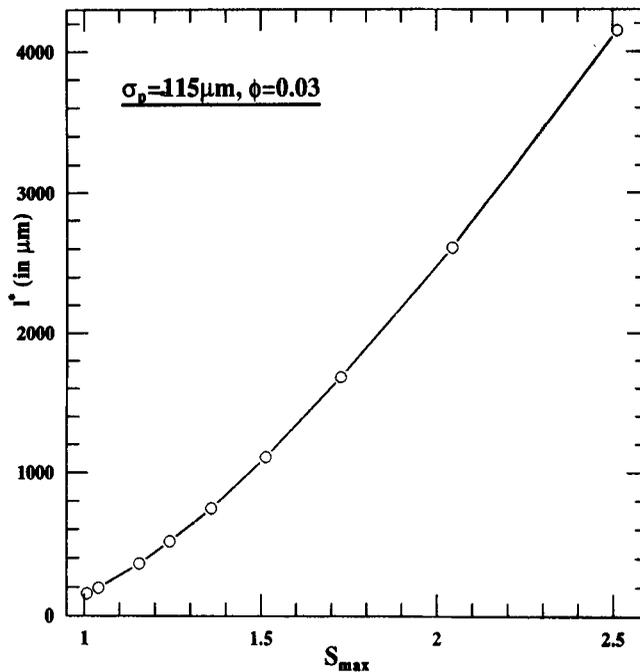

Figure 7. The calculated values of l^* (in μm) from the Mie theory (refer text) for different $S(q)$'s of figure 6 as a function of S_{max}, the first peak height of the $S(q)$.

that l^* increases almost linearly with the interaction. This qualitatively explains our results of the reduction of γ with the increase of the interaction strength.

5. Conclusions

In this paper, we have reported our observation of the formation of a crystalline phase when the interparticle interactions are increased in an equimolar binary mixture of polyball suspensions with a volume-fraction $\phi = 0.1$. In comparison, the interactions in the same binary system with $\phi = 0.2$ results in a metastable glassy state. This is in accord with our results in the BD simulations [13] of binary colloidal mixtures. We have also shown that the $g^{(1)}(t)$ of the binary mixture in the non-interacting fluid phases can be well-reproduced by replacing the τ_0 in the functional form of the correlation functions of the monodisperse suspensions by a properly weighted average τ_{eff} [eq. (13)], where l^* are calculated using Mie scattering theory. A model of the harmonically bound Brownian particle is used to calculate the root mean square displacements and the functional form of $g^{(1)}(t)$ suggested by MacKintosh and John [27] [eq. (9)] is shown to fit with a moderate success the results from the binary as well as monodisperse polyball suspensions while freezing into the crystalline or glassy states. These fits, though qualitative in nature due to the approximate form of (9), indicate that the parameter γ decreases as the particles in the suspensions start interacting with each other. This result is justified in the case of *monodisperse suspensions* by showing that the transport mean free path l^* which is inversely proportional to γ increases with the interaction between the particles. In conclusion, DWS has provided very interesting information on the dynamics of dense interacting colloids which can either form a crystalline state (at a low volume fraction) or a glassy state (at a high volume fraction). It could be worthwhile to carry out similar DWS experiments on binary colloids with different diameter ratios and relative volume fractions to map out the entire phase diagram.

Acknowledgements

Appendix

Within the Mie scattering theory [26], a general expression of l^* for monodisperse particles, is given by [21, 30, 31]

$$l^* = \frac{k_0^6 a_p^4}{\pi n_p \int_0^{2k_0 a_p} I(Q) Q^3 \, dQ} = \frac{(k_0 \sigma_p)^6 \sigma_p}{96 \phi \langle F(Q) S(Q) \rangle}. \tag{17}$$

Here n_p is the number density of particles and $\mathbf{Q} = (\mathbf{k}_0 - \mathbf{k}_f) a_p$ is the dimensionless momentum transfer for a single-scattering event. For monodisperse particles, we have replaced $I(Q)$ simply by the product of the form factor $F(Q)$ and the structure factor $S(Q)$. The angular brackets indicate an average over all the scattering paths. The form

factor $F(Q)$ for monodisperse systems is given by the Mie scattering theory as [26]

$$F(Qa_p) = Qa_p[A_1(\theta)A_1^*(\theta) + A_2(\theta)A_2^*(\theta)]. \tag{18}$$

where the dimensionless, single-scattering amplitudes $A_1(\theta)$ and $A_2(\theta)$ are related to the scattered far-fields E_ϕ and E_θ as

$$E_\phi = -\frac{ie^{ikr}}{kr}A_1(\theta)\sin\phi,$$

$$E_\theta = \frac{ie^{ikr}}{kr}A_2(\theta)\cos\phi,$$

$$A_1(\theta) = \sum_{n=1}^{\infty}\frac{2n+1}{n(n+1)}[a_n\pi_n(\cos\theta) + b_n\tau_n(\cos\theta)],$$

$$A_2(\theta) = \sum_{n=1}^{\infty}\frac{2n+1}{n(n+1)}[a_n\tau_n(\cos\theta) + b_n\pi_n(\cos\theta)], \tag{19}$$

with

$$\pi_n(\cos\theta) = \frac{P_n(\cos\theta)}{\sin\theta} \quad \text{and} \quad \tau_n(\cos\theta) = \frac{d}{d\theta}[P_n(\cos\theta)]. \tag{20}$$

The Mie scattering amplitudes are given by

$$a_n = \frac{\psi_n(\alpha)\psi_n^*(\beta) - m\psi_n(\beta)\psi_n^*(\alpha)}{\zeta_n(\alpha)\psi_n^*(\beta) - m\psi_n(\beta)\zeta_n^*(\alpha)},$$

$$b_n = \frac{m\psi_n(\alpha)\psi_n^*(\beta) - \psi_n(\beta)\psi_n^*(\alpha)}{m\zeta_n(\alpha)\psi_n^*(\beta) - \psi_n(\beta)\zeta_n^*(\alpha)},$$

where $\alpha = k_0 a_p$, $\beta = k_0 m a_p$, $\psi_n(x) = (\pi x/2)^{1/2}J_{n+1/2}(x)$ and $\zeta_n(x) = (\pi x/2)^{1/2}H_{n+1/2}^{(1)}(x)$ [$J_n(x)$ and $H_n(x)$ being the nth order Bessel function and Hermite polynomial, respectively] and $m^2 = \varepsilon_r = \varepsilon/\varepsilon_0$ is the relative dielectric constant of the sphere.

The static structure factor $S(Q)$ for the dense hard-spheres in the Percus–Yevick (PY) approximation is given in terms of the direct correlation function $c(Q)$ as [29,35]

$$S(Q) = \frac{1}{1 - n_p c(Q)},$$

$$c(Q) = 4\pi\int_0^{\sigma_p} r^2 c(r)\frac{\sin(Qr)}{Qr}dr,$$

$$c(r) = \alpha_0 + \alpha_1\left(\frac{r}{\sigma_p}\right) + \alpha_2\left(\frac{r}{\sigma_p}\right)^3,$$

$$\alpha_0 = -\frac{(1 + 2\phi)^2}{(1 - \phi)^4}, \tag{21}$$

$$\alpha_1 = \frac{6\phi(1 + \phi/2)^2}{(1 - \phi)^4},$$

$$\alpha_2 = \frac{1}{2}\phi\alpha_0.$$

References

[1] For a review, see A K Sood, in *Solid State Physics*, edited by H Ehrenreich and D Turnbull (Academic, New York, 1991) Vol. 45, p. 1

[2] E B Sirota, H D Ou-Yang, S K Sinha, P M Chaikin, J D Axe and Y Fujji, *Phys. Rev. Lett.* **62**, 1524 (1989)

[3] P N Pusey, W van Megen, P Bartlett, B J Ackerson, J G Rarity and S M Underwood, *Phys. Rev. Lett.* **63**, 2753 (1989)

[4] W van Megen and P N Pusey, *Phys. Rev.* **A43**, 5429 (1991)
W van Megen, S M Underwood and P N Pusey, *Phys. Rev. Lett.* **67**, 1586 (1991)
W van Megen and S M Underwood, *Phys. Rev.* **E47**, 248 (1993)

[5] P N Pusey and W van Megen, *Nature (London)* **320**, 340 (1986)
P N Pusey and W van Megen, *Phys. Rev. Lett.* **69**, 2083 (1987)
S E Paulin and B J Ackerson, *Phys. Rev. Lett.* **64**, 2663 (1990)
P N Pusey, *J. Phys. (Paris)* **48**, 709 (1987)
W van Megen and S M Underwood, *Langmuir* **6**, 35 (1990)

[6] S Yoshimura and S Hachisu, *Prog. Colloid Polym. Sci.* **68**, 59 (1983); *Nature (London)* **283**, 188 (1980)

[7] S Yoshimura and S Hachisu, *J. Phys. Colloq. (Paris)* **46**, C3-115 (1985)

[8] P Bartlett, R H Ottewill and P N Pusey, *J. Chem. Phys.* **93**, 1299 (1990); *Phys. Rev. Lett.* **68**, 3801 (1992)

[9] H M Lindsay and P M Chaikin, *J. Chem. Phys.* **76**, 3774 (1982)

[10] R Kesavamoorthy, A K Sood, B V R Tata and A K Arora, *J. Phys.* **C21**, 4737 (1988)

[11] A Meller and J Stavans, *Phys. Rev. Lett.* **68**, 3646 (1992)

[12] H Löwen, J P Hansen and J N Roux, *Phys. Rev.* **A44**, 1169 (1991)

[13] S Sanyal and A K Sood, *Phys. Rev. E* (in press); S Sanyal, Ph.D Thesis (IISc, Bangalore, India), Unpublished (1994)

[14] B V R Tata and A K Arora, *J. Phys. Condensed Matter* **4**, 7699 (1992)

[15] J F Sadoc and C N J Wagner, in *Glassy metals II*, edited by M Bech and H J Guntherödt, (Springer-Verlag, Berlin, 1983), p. 53
M Kimura and F Yonezawa, in *Topological disorder in condense matter*, edited by F Yonezawa and T Ninomiya (Springer-Verlag, Berlin, 1983) p. 80

[16] P N Pusey and R J A Tough, in *Dynamic light scattering: Applications of photon correlation spectroscopy*, edited by R Pecora (Plenum, New York, 1985)

[17] B J Berne and R Pecora, *Dynamic light scattering* (Wiley, New York, 1976)

[18] For reviews on MCT, see, W Götze, in *Liquids, freezing and the glass transition*, Proceedings of the Les Houches Summer School, Session L1, edited by J P Hansen, D Levesque and J Zinn-Justin, (North-Holland, Amsterdam, 1991), p. 287
W Götze and L Sjögren, *Rep. Prog. Phys.* **55**, 241 (1992)

[19] G Maret and P E Wolf, *Z. Phys.* **B65**, 409 (1987)
M Rosenbluh, M Hoshen, I Freund, M Kaveh, *Phys. Rev. Lett.* **58**, 2754 (1987)
I Freund, M Kaveh and M Rosenbluh, *Phys. Rev. Lett.* **60**, 1130 (1988)

[20] M J Stephen, *Phys. Rev.* **B37**, 1 (1988)
A A Golubentsev, *Zh. Eksp. Theor. Fiz.* **86**, 47 (1984); *Sov. Phys. JETP* **59**, 26 (1984)

[21] D J Pine, D A Weitz, P M Chaikin and E Herbolzheimer, *Phys. Rev. Lett.* **60**, 1134 (1988)

[22] D J Pine, D A Weitz, G Maret, P E Wolf, E Herbolzheimer and P M Chaikin in *Scattering and localization of classical waves in random media*, edited by P Sheng, (World Scientific, Singapore, 1989)
D J Pine, D A Weitz, J X Zhu and E Herbolzheimer, *J. Phys. France* **51**, 2101 (1990)

[23] S Sanyal, A K Sood, S Ramkumar, S Ramaswamy and N Kumar, *Phys. Rev. Lett.* **72**, 2963 (1994)

[24] P D Kaplan, A G Yodh and D J Pine, *Phys. Rev. Lett.* **68**, 393 (1992)

[25] Y Kuga and A Ishimaru, *J. Opt. Soc. Am.* **A8**, 831 (1984)
M P van Albada and A Lagendijk, *Phys. Rev. Lett.* **55**, 2692 (1985)

P E Wolf and G Maret, *Phys. Rev. Lett.* **55**, 2696 (1985)

E Akkerman, P E Wolf and R Maynard, *Phys. Rev. Lett.* **56**, 1471 (1986)

[26] A Ishimaru, *Wave propagation and scattering in random media* (Academic, New York, 1978), p. 29–30

H C van de Hulst, *Light scattering by small particles* (Dover, New York, 1957, 1981), p. 121–128, 176–177

[27] F C MacKintosh and S John, *Phys. Rev.* **B40**, 2383 (1989)

[28] G K Batchelor, *J. Fluid Mech.* **74**, 1 (1976); **131**, 155 (1983)

[29] N W Ashcroft and D C Langreth, *Phys. Rev.* **159**, 500 (1967)

J M Ziman, *Philos. Mag.* **6**, 1013 (1961)

[30] S Fraden and G Maret, *Phys. Rev. Lett.* **65**, 512 (1990)

[31] P D Kaplan, J L Rouke, A G Yodh and D J Pine, *Phys. Rev. Lett.* **72**, 582 (1994)

[32] F C MacKintosh, J X Zhu, D J Pine and D A Weitz, *Phys. Rev.* **B40**, 9342 (1989)

[33] S Sanyal *et al*, unpublished

[34] We thank Prof. A G Yodh for providing us with the computer program to calculate l^*

[35] W Hess and R Klein, *Adv. Phys.* **32**, 173 (1983) p. 181